Title
An Experimental Evaluation of the Received Signal from Blood at 50 MHz

Authors
Ferrara, K. Whittaker
Zagar, B.
Algazi, Ralph
et al.

Publication Date
1994

Peer reviewed

AN EXPERIMENTAL EVALUATION OF THE RECEIVED SIGNAL FROM BLOOD AT 50 MHz*

K. Whittaker Ferrara[1], B. Zagar[2], R. Algazi[2], R. Silverman[3], J. Sokil-Melgar[1]

[1]Riverside Research Institute, New York, NY, 10036, [2]CIPIC, University of California, Davis, CA 95616,
[3]Cornell University Medical College, New York, NY 10021

ABSTRACT

In order to evaluate the received echoes from blood at high frequencies, we present M-mode images as well as a statistical analysis of the in-vitro and in-vivo signal from blood using a short transmitted pulse with a transducer center frequency of 50 MHz. This analysis shows that individual scattering volumes can be tracked in the axial direction. Using both changes in the location and magnitude of the peak of the rf correlation, vessels as small as 100 microns can be visualized in the rf signal and distinguished from stationary targets. The experimental system provides the opportunity to examine changes in flow and in the vessel wall over a cardiac cycle.

I. INTRODUCTION

In order to evaluate the statistics of the backscattered signal from blood at high frequencies, a model for the received signal has been evaluated using in-vitro and in-vivo data. While previous researchers [1]-[3] have documented changes in the frequency dependence of the backscattered power from blood at frequencies above 30 MHz, the spatial and temporal correlation of the signal from these small sample volumes has not previously been evaluated. Our analysis shows that even for the sample volumes on the order of $100\mu m^3$, the concentration of red blood cells within the sample volume varies randomly and the peak of the rf correlation can be used to estimate velocity. Changes in both the location and magnitude of the peak of the correlation can be used to distinguish tissue from blood. The experimental baseband correlation of the signal also demonstrates the effect of lateral transit time. The experimental correlation exhibits extraneous peaks with an amplitude of 0.5, however.

Using this experimental methodology and wideband signal processing strategies, blood flow can be assessed in-vivo in small vessels near the transducer. This provides the opportunity to study physiologic phenomena on a very small scale. Clinical applications include the assessment of flow in the skin and lymphatic system and within anterior structures of the eye.

First, the signal correlation from in-vivo data acquired from the cephalic vein is evaluated. The effect of target motion on the correlation for this small sample volume is explored. Second, flow through a set of small vessels in the ciliary body of the rabbit is assessed. The examination of M-mode images, provides the opportunity to visualize flow in vessels as small as 100 μm, and using the wideband maximum likelihood estimate (WMLE) velocities as small as 0.4 mm/s in vessels of 120 μm are reliably estimated.

II. EXPERIMENTAL ENVIRONMENT

The received rf signal was digitized immediately after amplification. Statistical analysis and velocity estimation were performed in software. A Panametrics 5601AST pulser/ receiver with a 150 MHz bandwidth provided impulse excitation of a PVDF transducer. The received signal was amplified by 49 dB within the pulser/receiver. A LeCroy 4222 was used to provide an axial window and the signal then was digitized at 200 MHz. The timing of the pulser and the digitizer were not synchronized and therefore pulse to pulse jitter was removed by aligning the signal from stationary structures prior to the analysis. Other experimental parameters include:

1051-0117/94/0000-1603 $4.00 © 1994 IEEE

Transducer - Panametrics	P150-2-F0.50
Transducer aperture	6 mm
Focal length	12 mm
3dB Bandwidth of received signal	10-50 MHz
Center Frequency of received signal	38 MHz
One sided 6 dB lateral beam width	40 μm
Pulse Repetition Rate	1000 Hz

III. RESULTS AND DISCUSSION

In order to establish the accuracy of velocity estimation with this experimental system, a flow phantom was constructed, and used to measure the velocity profile in a single fiber with an inner diameter of 200 μm. The results of these experiments are reported in [5]. Velocities of 2-5 mm/s were accurately estimated, as verified by the flow rate for the known experimental conditions.

M-mode images are presented, and the data included in these images is used to determine the statistics of the received signal and to evaluate the performance of velocity estimation strategies. In the M-mode images, the signal from increasing depth is shown as an intensity modulated trace along the horizontal axis, and the signal from sequential individual pulses is stacked along the vertical axis. In this format, echoes from stationary objects appear as vertical stripes. A well-defined echo complex from an aggregate of scatterers results in a series of tilted lines that can be tracked in depth and time. Scatterers moving away from the transducer (increasing in depth) exhibit lines that shift to an increasing depth with each pulse. Thus, faster moving scatterers produce a pattern that approaches the horizontal, while slower scatterers produce a pattern that approaches the vertical structure of the fixed vessel wall. The structured pattern from an individual group will begin to blur as these scatterers leave the sample volume, or as they become mixed with other red blood cells due to a velocity gradient within the sample volume. The time interval over which groups of scatterers move together can be estimated by evaluating the vertical dimension with a distinct amplitude. This provides a gross estimate of the correlated signal interval.

Two sets of in-vivo experiments were then conducted in order to study the properties of the received signal from blood interrogated with this wideband high-frequency transducer. We first present an analysis of the signal from the human cephalic vein, in order to evaluate the statistics of the signal from blood within a large vessel. Second, data from the ciliary body of a rabbit are presented to provide the opportunity to evaluate the signal from a region with multiple small vessels.

CEPHALIC VEIN

Figure 1 shows a portion of the M-mode image from the cephalic vein in which the rf signal has been detected, the contrast has been enhanced and the time axis has been interpolated by a factor of 2. The position of the vessel wall is indicated in Figure 1 as well as regions of blood scatterers. The diameter of the vessel is slightly less than 4 mm, with the transducer focus placed at the near vessel wall. Figure 1 includes a depth of approximately 1.8 mm. At depth D1, the motion of a group of scatterers through the lateral beam width can be observed with the axial motion producing the diagonal slant, and the lateral motion producing the changes in the gray level along one individual diagonal.

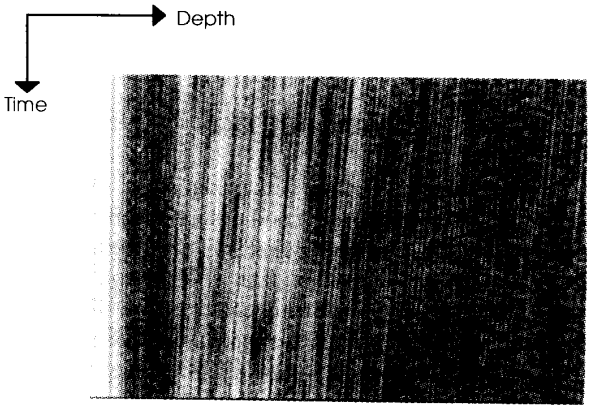

Figure 1. Detected M-mode image of human cephalic vein

EVALUATION OF THE SIGNALCORRELATION

The experimental correlation between the signal arriving after a delay of time t_0 and the signal arriving after a delay $t_0+\tau+nT$, where n is a integer and T is the pulse repetition period, is studied as a function of τ and n. The correlation before

averaging over additional received pulses is determined by (1), termed the finite average autocorrelation

$$C(t_o, t_o + \tau; n) = \sum_{k=0}^{N-|n|-1} 1 / (N - |n|) \int_{t0}^{t0 + W} r_k'(t + t_o)a(t + t_o) \cdot r_{k+n}'^{*}(t + t_o + \tau)a(t + t_o + \tau)dt \quad (1)$$

where $r_k'(t)$ is the baseband return from the kth pulse, a(t) represents the axial window, t_0 is a temporal offset where $0 < t_0 < T$, and N is chosen to equal the maximum value of n. The correlation was evaluated for the experimental data after interpolation of the data by a factor of two, demodulation with the 38 MHz center frequency, a low pass filter with a cutoff frequency of 20 MHz, and clutter rejection. A rectangular axial window of 20 samples (approximately twice the acoustic wavelength) is used in this analysis, although the results do not change significantly with an increase in the window to a maximum of 40 samples. A high pass FIR filter of order 50 was applied to the data to remove the stationary clutter, implemented as an estimation- subtraction filter. The zero frequency component is estimated and removed through subtraction.

The correlation is normalized by the averaged correlation at lag zero and pulse period zero for each position, which is given by:

$$C(t_o, t_o) = 1 / N \sum_{k=0}^{N-1} \int_{t0}^{t0 + W} r_k'(t + t_o)a(t + t_o) \cdot r_k'^{*}(t + t_o)a(t + t_o)dt \quad (2)$$

Since changes in the correlation magnitude over the entire data set are hypothesized to be an important factor in the detection of flow at beam-vessel angles which approach ninety degrees, this single normalization factor is applied to data from each fixed starting depth. The following figure shows the magnitude of the normalized correlation of the baseband envelope of the raw rf data. In the experimental evaluation of the correlation, the signal from an axial region whose size is on the order of the sample volume, is correlated with the signal from other axial regions and from other received pulses. Using the above notation, the normalized correlation function ((1) divided by (2)), is denoted $C(t_o, t_o + \tau, n) / C(t_o, t_o)$, where t_o varies with the starting depth of interest. The normalized correlation estimate is then plotted in three dimensions as a function of τ and n.

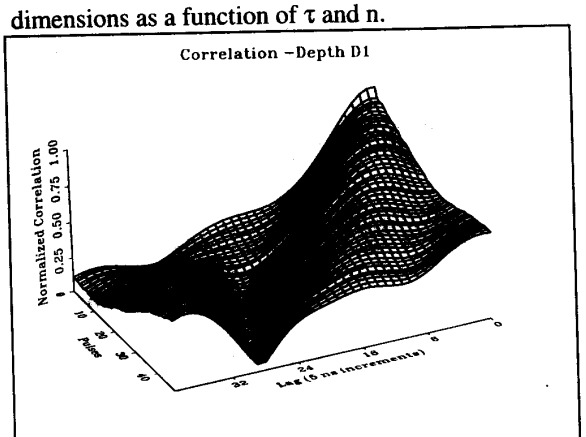

Figure 2. Baseband correlation of the signal from depth D1 in the cephalic vein image presented as Figure 1.

Figure 2 shows the correlation of the signal at depth D1. The motion of scatterers within the sample volume is shown by the shift of the peak of Figure 2. At depth D1, the peak has a normalized height of 0.42 after 49 pulses and is located at lag 16, corresponding to a peak of 0.62 mm/s. The one sided width of the correlation at a lag of zero periods is 27.5 ns, corresponding to a single cycle at a center frequency of 36.4 MHz. Therefore, for this transducer with an estimated center frequency of 38 MHz, the one-sided correlation width is approximately equal to the length of the impulse response of the transducer. Assuming that this reduction to a normalized correlation of 0.42 approximately indicates the lateral transit time of scatterers across the beam width of 40 μm, the angle between the transducer axis and the axis of the blood vessel is predicted to be 50 degrees. The angle between the skin surface and the transducer axis was measured as 40 degrees. We note that additional correlation peaks of an approximate height of 0.5 are present over a range of periods.

SMALL VASCULATURE- RABBIT CILIARY BODY

In order to evaluate the spatial and velocity resolution of the system for a second case of interest, we have evaluated blood flow within the ciliary body of the rabbit eye. This is a highly muscular structure with blood flow provided by the

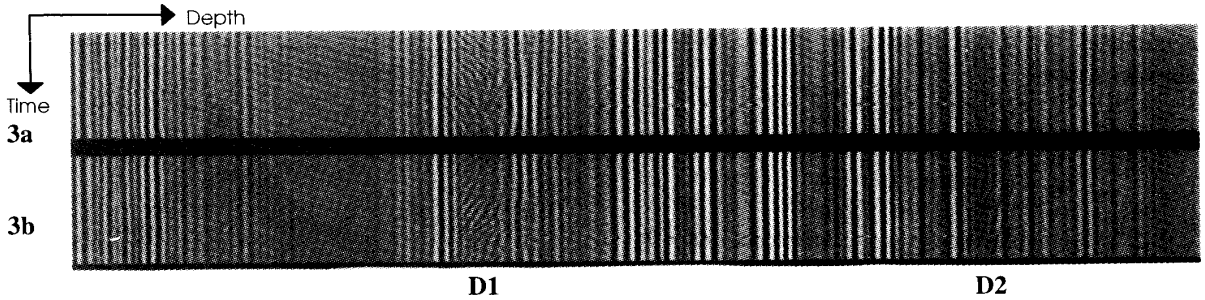

Figures 3a and 3b. Rf M-mode image of rabbit ciliary body

ciliary arterial system. The rabbit was anesthetized and the eye proptosed in preparation for the experiment.

Figures 3a and 3b present M-mode images obtained at two separate times from vasculature within the ciliary body. Within each image are 128 lines acquired at the pulse repetition rate of 1 kHz. The largest vessel is located at depth D1, with an

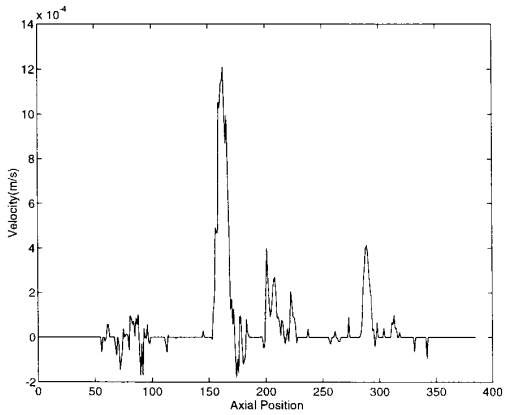

Figure 4. WMLE of the velocity within the ciliary body data shown in Figure 3a.

approximate diameter of 180 μm and flow is clearly visualized from the slanted stripes within the image. Motion of the vessel walls can also be observed over each set of 128 pulses, where each represents a fraction of the cardiac cycle. The two data sets presented in Figures 3a and 3b were obtained at different portions of the cardiac cycle, with a reversal in flow direction occurring between these two times.

The velocity at each point within the image was then estimated and the resulting time and depth dependent information is summarized in Figures 4-5. The velocity for depths within Figure 4 is presented as a function of axial position, with each increment corresponding to 7.42 μm. The data were demodulated and a low pass filter was applied. Two third-order Chebychev IIR step-initialized wall filters were then applied to the data, with the cutoff velocity ranging from 0.02 mm/s to 0.14 mm/s. The results presented in Figures 4-5 were obtained with a wall filter with a cutoff velocity of 0.06 mm/s. The results for different wall filter cutoff velocities are summarized in [1]. As the filter cutoff velocity is decreased below 0.06 mm/s, it is difficult to distinguish motion of the vessel walls and blood flow.

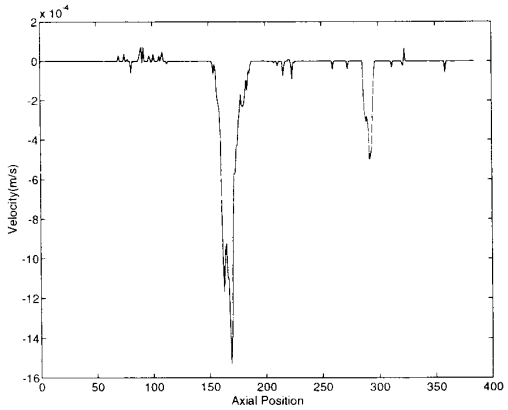

Figure 5. WMLE of the velocity within the ciliary body for the data shown in Figure 3b.

The velocity was estimated using the wideband maximum likelihood estimator (WMLE) [5] with the returned signal from 20 pulses coherently summed in each estimate. Twenty six velocity estimates were made at each axial position within each file. The average velocity over the 128 ms interval is presented in Figures 4-5. Following velocity estimation, the normalized likelihood was

compared to a threshold of 0.65 and the post-wall filtered signal power was compared with an absolute power threshold. The velocity was set to zero in regions in which these values fell below the threshold.

The velocity estimate for the vessel at depth D1 in Figure 3 appears at axial position 160 in Figures 4 and 5. The velocity estimate for the vessel at depth D2 in Figure 3 appears at axial position 290 in Figures 4 and 5. The reversal in flow direction between Figures 3a and 3b is clearly shown in the change in the sign of the velocity at positions 160 and 290. The average estimated velocity for depth D1 is 1.2 mm/s for the data presented in Figure 3a and -1.5 mm/s for the data presented in Figure 3b, at these two times within the cardiac cycle. The average estimated velocity for depth D2 is 0.4 mm/s for the data presented in Figure 3a and -0.5 mm/s for the data presented in Figure 3b, at these two times within the cardiac cycle.

IV. CONCLUSION

The correlation of the received signal from the cephalic vein shows that the width of the correlation for data acquired from a single pulse is approximately predicted by the impulse response of the transducer. The shift in the peak of the correlation predicts a velocity of 0.62 mm/s. The signal remains correlated for a time interval which is predicted by the transit time, as estimated from the lateral beam width, beam-vessel angle and axial velocity. The correlation demonstrates additional peaks which may be produced by noise and by a non-zero correlation between different scattering regions.

Blood flow through vessels with a size of 120 microns and a peak velocity of 0.4 mm/s can be visualized in-vivo. Flow through small vessels with lower volume flow rates can be visualized, but detection of this flow is difficult due to the motion of the vessel walls. This experimental system provides the opportunity to examine changes in the vasculature over a cardiac cycle in-vivo. Changes in the vessel diameter, velocity, and wall echogenicity are observed over a cardiac cycle. Further studies will be conducted to evaluate these changes and phenomena.

V. REFERENCES

[1] G. R. Lockwood, L. K. Ryan, J. W. Hunt, and F. S. Foster, "High frequency ultrasound vascular tissue characterization," *Ultrasonics Symposium Proceedings*, Vol. 3, pp. 1409-1412, 1990.

[2] G. R. Lockwood, L. K. Ryan, J. W. Hunt, and F. S. Foster, "Measurement of the Ultrasonic Properties of Vascular Tissues and Blood from 35-65 MHz," *Ultrasound in Medicine and Biology*, Vol. 17, No. 7, pp. 653-666, 1991.

[3] M. G. M. de Kroon, C. J. Slager, W. J. Gussenhoven, P. W. Serruys, J. R. T. C. Roelandt, and N. Bom, "Cyclic changes of blood echogenicity in high-frequency ultrasound," *Ultrasound Med. & Biol.*, Vol. 17(7), pp. 723-728, 1991.

[4] K. Ferrara, B. Zagar and V.R. Algazi, "Theoretical and Experimental Evaluation of the Received Signal from Blood at High Frequencies, in preparation for *IEEE Transactions on Ultrasonics, Ferroelectrics and Frequency Control*.

[5] K.W. Ferrara and V.R. Algazi. "A New Wideband Spread Target Maximum Likelihood Estimator For Blood Velocity Estimation Part One-Theory," *IEEE Transactions on Ultrasonics, Ferroelectrics and Frequency Control*, January 1991, pp. 1-16.

*ACKNOWLEDGMENTS

The authors acknowledge the support of the National Science Foundation grant BCS-9108940, the Whitaker Foundation and National Institutes of Health grants HL48273, CA60681 and EY01212.